


# Reproducibility of dynamic contrast-enhanced MRI and dynamic susceptibility contrast MRI in the study of brain gliomas: a comparison of data obtained using different commercial software

Gian Marco Conte<sup>1</sup> · Antonella Castellano<sup>1</sup> · Luisa Altabella<sup>1,2</sup> · Antonella Iadanza<sup>1</sup> · Marcello Cadioli<sup>1,3</sup> · Andrea Falini<sup>1</sup> · Nicoletta Anzalone<sup>1</sup> 

Received: 21 September 2016 / Accepted: 19 December 2016 / Published online: 9 January 2017  
© Italian Society of Medical Radiology 2017

## Abstract

**Purpose** Dynamic susceptibility contrast MRI (DSC) and dynamic contrast-enhanced MRI (DCE) are useful tools in the diagnosis and follow-up of brain gliomas; nevertheless, both techniques leave the open issue of data reproducibility. We evaluated the reproducibility of data obtained using two different commercial software for perfusion maps calculation and analysis, as one of the potential sources of variability can be the software itself.

**Methods** DSC and DCE analyses from 20 patients with gliomas were tested for both the intrasoftware (as intraobserver and interobserver reproducibility) and the intersoftware reproducibility, as well as the impact of different post-processing choices [vascular input function (VIF) selection and deconvolution algorithms] on the quantification of perfusion biomarkers plasma volume (Vp), volume transfer constant ( $K^{\text{trans}}$ ) and rCBV. Data reproducibility was evaluated with the intraclass correlation coefficient (ICC) and Bland–Altman analysis.

**Results** For all the biomarkers, the intra- and interobserver reproducibility resulted in almost perfect agreement in each

software, whereas for the intersoftware reproducibility the value ranged from 0.311 to 0.577, suggesting fair to moderate agreement; Bland–Altman analysis showed high dispersion of data, thus confirming these findings. Comparisons of different VIF estimation methods for DCE biomarkers resulted in ICC of 0.636 for  $K^{\text{trans}}$  and 0.662 for Vp; comparison of two deconvolution algorithms in DSC resulted in an ICC of 0.999.

**Conclusions** The use of single software ensures very good intraobserver and interobservers reproducibility. Caution should be taken when comparing data obtained using different software or different postprocessing within the same software, as reproducibility is not guaranteed anymore.

**Keywords** Gliomas · Perfusion weighted MRI · Dynamic susceptibility contrast MRI (DSC) · Dynamic contrast-enhanced MRI (DCE) · Reproducibility of findings · Vascular input function (VIF)

## Abbreviations

DSC	Dynamic susceptibility contrast
DCE	Dynamic contrast-enhanced
Vp	Plasma volume
$K^{\text{trans}}$	Volume transfer constant
VIF	Vascular input function
SVD	Singular value decomposition
ICC	Intraclass correlation coefficient

**Electronic supplementary material** The online version of this article (doi:10.1007/s11547-016-0720-8) contains supplementary material, which is available to authorized users.

✉ Nicoletta Anzalone  
anzalone.nicoletta@hsr.it

<sup>1</sup> Neuroradiology Unit and CERMAC, San Raffaele Scientific Institute and Vita-Salute San Raffaele University, via Olgettina 60, 20132 Milan, Mi, Italy

<sup>2</sup> Department of Medical Physics, San Raffaele Scientific Institute, via Olgettina 60, 20132 Milan, Mi, Italy

<sup>3</sup> Philips Healthcare, via Gaetano Casati 23, 20900 Monza, MB, Italy

## Introduction

Dynamic susceptibility contrast MRI (DSC) and Dynamic contrast-enhanced MRI (DCE) can be useful tools in the diagnosis and follow-up of brain gliomas. Most studies published on this topic used perfusion-derived biomarkers

for gliomas grading [1–5], patients' outcome prediction [6–11] and differentiation of tumor recurrence from treatment-related effects like radionecrosis and pseudoprogression [12–16].

However, reproducibility is still an open issue for both techniques: no standardized protocol for acquisition and analysis of perfusion techniques is still available and, consequently, different research groups have used different protocols, generating a wide range of results [17–22]. Recently some steps towards standardization have been made, with the publication of an evidence- and consensus-based standards document for DCE [23] and a white paper for DSC [24].

One of the potential sources of variability is the software chosen for perfusion map calculation and analysis [25–32] since each software implements different analysis tools [i.e. leakage correction for DSC maps or automatic detection of vascular input function (VIF)] and sometimes different algorithms.

The aim of this study was to test the reproducibility of data obtained from studying the same cohort of patient with two commercial software, which were chosen based on the rationale that they could be used independently from the MR machine available for the acquisition, thus reducing data spread and improving standardization of perfusion analysis. We tested both intrasoftware (including the intraobserver and interobservers reproducibility) and inter-software reproducibility and the impact of different post-processing choices, such as VIF selection methods and deconvolution algorithms, on the quantification and reproducibility of perfusion biomarkers obtained from DSC and DCE analyses.

## Methods

### Patients

DCE and DSC data derived from 20 patients (mean age 51 years; range 16–76 years; 10 M/10 F) with histologically confirmed gliomas (8 WHO II, 4 WHO III and 8 WHO IV) were retrospectively evaluated. This study was approved by the ethical committee of our Institution.

### MR imaging

MR imaging was performed on a 3T scanner (Achieva, Philips Healthcare, Best, The Netherlands) equipped with 80 mT/m gradients using a phased-array head 8 channel-coil. Online Resource 1 summarizes the imaging parameters of the MRI sequence protocol.

DCE–MRI was performed with a dynamic gradient-echo  $T1$ -weighted sequence using the following parameters:

TR/TE 3.9/1.8 ms; flip angle 15°; matrix 96 × 84; FOV 230 × 201 mm; section thickness, 2.5 mm; in-plane acquisition voxel size, 2.4 × 2.4 mm. Seventy dynamic scans were performed with a temporal resolution of 5.1 s. The total acquisition time for DCE–MRI was 6 min and 10 s. DCE–MRI was preceded by a variable flip angle (VFA) axial sequence for  $T1$  mapping.

DSC–MRI was performed with an axial gradient-echo  $T2^*$ -weighted EPI sequence using the following parameters: TR/TE 1500/40 ms; flip angle 75°; matrix 96 × 77 mm; FOV 230 × 230 mm; section thickness, 5 mm; in-plane acquisition voxel size, 2.4 × 2.9. Eighty dynamic scans were performed with a temporal resolution of 1.5 s. The total acquisition time for DSC–MRI was 2 min and 4 s.

A cumulative fixed dose of 10 ml of gadobutrol (Gadovist, 1 mmol/ml; Bayer Schering Pharma, 6 Berlin, Germany) was administered, splitted in two boluses of 5 ml. The first bolus of 5 ml was injected 50 s after the start of the DCE sequence using a power injector (Spectris Solaris MR injector; MedRad, Indianola, Pennsylvania) at a rate of 2 ml/s, immediately followed by a 20 ml continuous saline flush at the same injection rate. The second bolus of 5 ml was injected 16 s after the start of the DSC sequence using the same power injector at a rate of 5 ml/s, followed by a 20 ml saline flush at the same injection rate. Thus, the contrast administration during DCE sequence pre-saturated the tissue for the following DSC–MR imaging.

### Preprocessing

Perfusion MR analysis was performed using Olea Sphere (v. 2.3, Olea Medical Solutions, La Ciotat, France) and NordicIce (v. 2.3.12, NordicNeuroLab, Bergen, Norway). In both software, preprocessing steps included automatic motion correction by a rigid-body registration, automatic spatial smoothing and background segmentation.

### DCE analysis

For DCE analysis, patient-specific baseline  $T1$  maps were derived from VFA axial sequences (see Online Resource 1 for acquisition details).

In both software DCE analysis was based on the extended Tofts model [33]. In NordicIce, a venous VIF was obtained by manually drawing a ROI in the superior sagittal sinus (SSS). In Olea Sphere both a manual venous VIF and an automatic one were obtained; the venous one was obtained from the SSS, while the automatic one was obtained using a tool implemented in the software [34], which selected both arteries and veins as sources of input. Parametric maps of volume transfer constant ( $K^{trans}$ ) and plasma volume ( $V_p$ ) were then obtained.

## DSC analysis

In both software, DSC analysis was performed using the singular value decomposition (SVD) algorithm for deconvolution [35]. However, while Olea Sphere offers different methods for SVD, and both the standard truncated SVD (sSVD) and oscillation-index cSVD (oSVD) were used for analysis, in NordicIce only sSVD was available. An arterial VIF was obtained in Olea Sphere using an automatic method [34] while in NordicIce it was obtained semi-automatically: the observer selected the axial slice of interest and then the software searched for a valid vascular signal. Leakage correction was not applied during the postprocessing since it was already obtained with the contrast administration during the DCE acquisition, which served as a pre-bolus. Parametric maps of cerebral blood volume (CBV) were then obtained.

A fixed hematocrit value of 0.45 was set in both software.

## Image analysis

All the parametric maps were independently analyzed by two observers (GMC, with 3 years experience in perfusion analysis, NA with 7 years experience in perfusion analysis).

In both software, perfusion maps were automatically co-registered with FLAIR and/or post-contrast T1 images by performing a rigid transformation of the datasets.

For each parametric map, multiple circular ROIs, 25–30 mm<sup>2</sup> in area, were drawn in the tumor area that showed the highest value of perfusion biomarkers, then the one showing the highest mean value for each perfusion biomarker was selected. To normalize CBV values, a single elliptic ROI, 250–300 mm<sup>2</sup> in area, was drawn in the contralateral normal appearing white matter (NAWM) in the *centrum semiovale* (nCBV). The ratio (rCBV) between the tumor-CBV and nCBV was then considered. The analysis was repeated after one month to assess intraobserver reproducibility.

From DCE analysis, for each parametric map and each observer three datasets were obtained: one with the automatic VIF selection (Olea automatic) and two with the manual VIF selection (Olea Manual and NordicIce); from DSC two datasets (Olea automatic and NordicIce) were obtained.

Moreover, to avoid any possible variability due to different ROIs positioning between observers, intersoftware reproducibility was re-tested drawing the ROIs in the same tumor area in the two software. To do so, co-registered anatomical series were used as reference to guarantee the same ROIs positioning in the two software. Mean value of selected ROIs was then used for the comparison.

To test the impact of different postprocessing options on the quantitative data, additional analyses were performed using Olea Sphere: for DCE, the reproducibility of data obtained using the automatic and the manual VIF selection and for DSC the data obtained using the sSVD and oSVD methods. For all these analyses, the ROIs positions were kept constant.

## Statistical analysis

Intraclass Correlation Coefficient analysis (ICC) selecting a two-way random effect model was performed to assess intra- and intersoftware reproducibility using SPSS (SPSS 20.0 for MacOSX, IBM, Chicago, IL, USA) and interpreted as follows: 0–0.2 indicates poor agreement, 0.3–0.4 indicates fair agreement, 0.5–0.6 indicates moderate agreement, 0.7–0.8 indicates strong agreement and >0.8 indicates almost perfect agreement.

Additionally, to compare data obtained with the two software and with the different postprocessing options, Bland–Altman analysis was performed using Graph Pad Prism 6 (GraphPad Software, La Jolla, California, USA, <http://www.graphpad.com>).

## Results

### Intrasoftware reproducibility

Intraobserver reproducibility resulted in an ICC always superior than 0.8 except for two comparisons (Table 1). Similar results were obtained for interobservers agreement (Table 1).

### Intersoftware reproducibility

Intersoftware reproducibility resulted fair to moderate for all perfusion biomarkers (Table 2): ICC ranged from 0.354 to 0.577; similar result was found drawing the ROIs in the same tumor area in the two software (Table 3). Selecting the same SVD algorithm in the two software only slightly improved reproducibility of rCBV (Table 3).

Graphs derived from Bland–Altman analysis are summarized in Fig. 1; when comparing Olea Automatic and NordicIce, bias for  $K^{trans}$ , Vp and rCBV were 0.0035, –0.8030 and –4.604 while 95% limits of agreement range were (–0.16, 0.17), (–8.6, 6.99), (–17.29, 8.07), respectively; comparing Olea Manual and NordicIce, bias for  $K^{trans}$  and Vp were 0.0210 and –0.4285 while 95% limits of agreement range were (–0.09, 0.13) and (–6.62, 5.76), respectively.

**Table 1** ICC values for intraobserver and interobserver reproducibility

Parameter	Olea automatic	Olea manual	NordicIce
<i>K</i> <sup>trans</sup>			
Observer A1 vs A2	0.986 (CI 0.96–0.99)	0.980 (CI 0.95–0.99)	0.736 (CI 0.44–0.88)
Observer B1 vs B2	0.999 (CI 0.99–1.00)	0.984 (CI 0.96–0.99)	0.923 (CI 0.81–0.96)
Observer A1 vs B1	0.996 (CI 0.99–1.00)	0.970 (CI 0.89–0.99)	0.859 (CI 0.68–0.94)
Observer A2 vs B2	0.984 (CI 0.96–0.99)	0.963 (CI 0.91–0.98)	0.829 (CI 0.61–0.92)
<i>V</i> <sub>p</sub>			
Observer A1 vs A2	0.994 (CI 0.98–0.99)	0.966 (CI 0.91–0.98)	0.804 (CI 0.57–0.91)
Observer B1 vs B2	0.993 (CI 0.98–0.99)	0.973 (CI 0.93–0.98)	0.935 (CI 0.84–0.97)
Observer A1 vs B1	0.985 (CI 0.96–0.99)	0.924 (CI 0.81–0.96)	0.848 (CI 0.66–0.93)
Observer A2 vs B2	0.994 (CI 0.98–0.99)	0.970 (CI 0.87–0.99)	0.849 (CI 0.66–0.93)
<i>rCBV</i>			
Observer A1 vs A2	0.891 (CI 0.74–0.95)	–	0.702 (CI 0.38–0.87)
Observer B1 vs B2	0.984 (CI 0.96–0.99)	–	0.897 (CI 0.76–0.95)
Observer A1 vs B1	0.919 (CI 0.78–0.96)	–	0.903 (CI 0.77–0.96)
Observer A2 vs B2	0.912 (CI 0.78–0.96)	–	0.790 (CI 0.54–0.91)

Letters (A, B) refers to observers, numbers (1, 2) refers to the different timepoints

*K*<sup>trans</sup> volume transfer constant, *V*<sub>p</sub> plasma volume, *rCBV* relative cerebral blood volume, *ICC* intraclass correlation coefficient, *CI* 95% confidence interval

**Table 2** ICC values for intersoftware reproducibility

Parameter	Olea automatic vs NordicIce	Olea manual vs NordicIce
<i>K</i> <sup>trans</sup>	0.311 (CI –0.16–0.66) <sup>a</sup>	0.525 (CI 0.14–0.77) <sup>a</sup>
<i>V</i> <sub>p</sub>	0.404 (CI –0.03–0.71) <sup>a</sup>	0.504 (CI 0.08–0.77) <sup>a</sup>
<i>rCBV</i>	0.577 (CI 0.12–0.81) <sup>b</sup>	–

*K*<sup>trans</sup> volume transfer constant, *V*<sub>p</sub> plasma volume, *rCBV* relative cerebral blood volume, *ICC* intraclass correlation coefficient, *CI* 95% confidence interval

<sup>a</sup> NordicIce used with manual selection of VIF in SSS

<sup>b</sup> *rCBV* obtained with oSVD method in Olea Sphere and sSVD method in NordicIce

**Impact of postprocessing options on reproducibility**

Reproducibility of different VIF selection methods for DCE-derived biomarkers resulted in an ICC of 0.636 for *K*<sup>trans</sup> and 0.662 for *V*<sub>p</sub> (Table 4). Regarding Bland–Altman

analysis (Fig. 1), bias for *K*<sup>trans</sup> and *V*<sub>p</sub> were –0.0175 and –0.3745 while 95% limits of agreement range were (–0.16, 0.12) and (–6.50, 5.75), respectively.

Comparison of the two SVD methods for DSC resulted in an ICC of 0.999 for *rCBV* in the same software (Table 4).

**Discussion**

One of the major limitations to the use of PWI in the diagnostic workflow of brain tumors is the lack of standardization of acquisition and analysis protocols [17–20]. This leads to highly heterogeneous findings among studies, thus decreasing reproducibility. Some of the known PWI analysis variables are operator-dependent, such as the VIF selection [17, 18, 25, 26, 28] and ROI positioning [20].

Another source of variability is the choice of the PWI analysis software itself [25–32]: different FDA and CE-approved software are available, such as the software

**Table 3** ICC values for intersoftware reproducibility evaluated with fixed ROI

Parameter	Olea automatic vs NordicIce	Olea manual vs NordicIce	Olea automatic (sSVD) vs NordicIce (sSVD)
<i>K</i> <sup>trans</sup>	0.354 (CI –0.11–0.69) <sup>a</sup>	0.514 (CI 0.09–0.78) <sup>a</sup>	–
<i>V</i> <sub>p</sub>	0.446 (CI –0.01–0.74) <sup>a</sup>	0.575 (CI 0.17–0.81) <sup>a</sup>	–
<i>rCBV</i>	0.455 (CI –0.08–0.79) <sup>b</sup>	–	0.582 (CI 0.005–0.843)

*K*<sup>trans</sup> volume transfer constant, *V*<sub>p</sub> plasma volume, *rCBV* relative cerebral blood volume, *ICC* intraclass correlation coefficient, *CI* 95% confidence interval

<sup>a</sup> NordicIce used with manual selection of VIF in SSS

<sup>b</sup> *rCBV* obtained with oSVD method in Olea Sphere and sSVD method in NordicIce

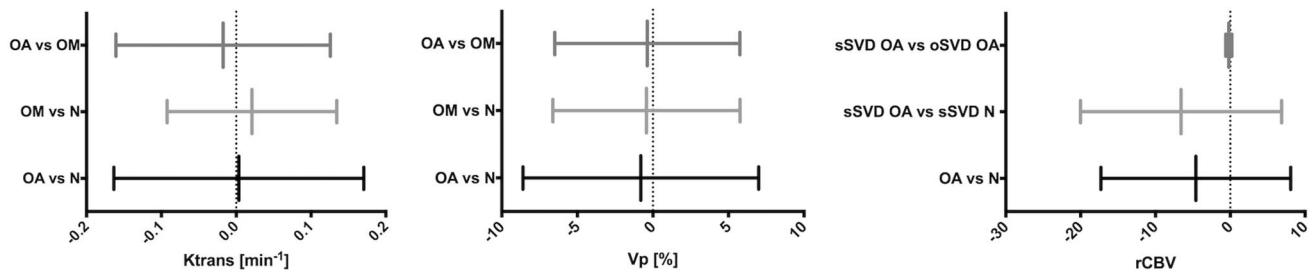


**Fig. 1** Summary of Bland–Altman analysis for  $K^{trans}$ ,  $V_p$  and  $rCBV$ . For each horizontal bar the central line corresponds to bias, while the left and right ends represent the limits of agreement. The bar length is

proportional to the dispersion of data. *OA* Olea automatic, *OM* Olea manual, *N* Nordiclce

**Table 4** ICC values for impact of postprocessing options on reproducibility. All analyses performed using the same software (Olea Sphere)

Parameter	Automatic VIF vs manual VIF	oSVD vs sSVD
$K^{trans}$	0.636 (CI 0.29–0.83)	–
$V_p$	0.662 (CI 0.31–0.85)	–
$rCBV$	–	0.999 (CI 0.98–1.00)

$K^{trans}$  volume transfer constant,  $V_p$  plasma volume,  $rCBV$  relative cerebral blood volume, *ICC* intraclass correlation coefficient, *CI* 95% confidence interval

platforms offered by all the major MR manufacturers, and some commercial software packages for advanced MR imaging analyses. Moreover, especially in neuroimaging, some groups analyze PWI datasets using non CE and FDA approved in-house software.

The issue of the reproducibility of data derived from different software seems to be independent from imaging technique and anatomical district: previous studies focused on data obtained using different software or different versions of the same software in both CT-PWI [27, 29, 30] and MR-PWI [25, 26, 28, 31, 32]. To our best knowledge, this study is the first reporting data on DCE reproducibility in brain imaging.

**Intrasoftware reproducibility**

Regarding the intrasoftware analysis, we found good reproducibility for all comparisons (Table 1). One of the two software, Olea Sphere, showed narrower and higher range of ICC values (Fig. 2). Better reproducibility was especially observed when the automatic selection of VIF was used, probably because this method avoids one of the possible observer-dependent variables. Nevertheless, our data shows that the manual selection of VIF also ensures a good intrasoftware reproducibility when selected in a fixed position (in our study, the superior sagittal sinus).

Slight differences were found in DCE and DSC reproducibility:  $V_p$  and  $K^{trans}$  showed slightly better results compared to  $rCBV$  for both intraobserver and interobserver reproducibility (Table 1; Fig. 2); this may be due to the need of drawing two ROIs for  $rCBV$  estimation, one in the tumor area, and one in the NAWM, thus adding an additional variable compared to  $K^{trans}$  and  $V_p$ .

**Intersoftware reproducibility**

Regarding the intersoftware analysis, the ICC values obtained suggest only fair to moderate reproducibility for

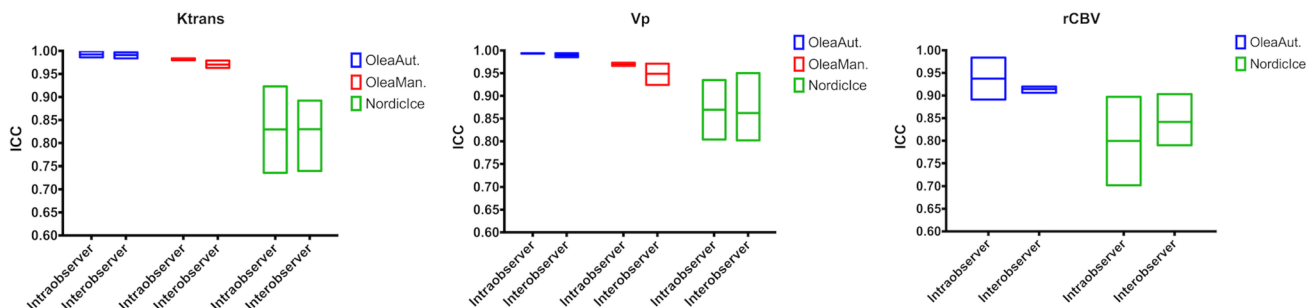


**Fig. 2** ICC values of intrasoftware reproducibility for  $K^{trans}$ ,  $V_p$  and  $rCBV$ . Summary of ICC values obtained in all comparisons; upper and lower limits of the box represent the highest and lowest ICC value obtained; the central line represents the mean ICC value obtained



both DSC and DCE parameters; moreover, the 95% confidence interval for ICC values showed a wide range of results for all comparisons (Table 2). This ICC value dispersion suggests that even if the two software were used with similar parameters, some differences do exist in how the two software generate the perfusion maps, and are probably due to options inaccessible to the users.

Similar results were also obtained drawing the ROIs in the same tumor area in the two software, with only a slight improvement of ICC values, showing that ROIs positioning might not be a major issue for PWI reproducibility if the analysis is performed by trained readers (Table 3).

The Bland–Altman analysis confirmed this data, since the limits of agreement and the dispersion of data were too wide to define the results reproducible (Fig. 1); the automatic VIF selection seems to slightly underestimate parameters if compared to the manual method; this may be due to the different composition of the input of

the automatic method (see Sect. “VIF selection in DCE” paragraph).

Slight differences in DSC and DCE reproducibility were found when different methods of VIF selection were applied in the two software for DCE analysis, obtaining better results for rCBV (Tables 2, 3); these differences disappeared when the manual selection of VIF was applied in both software for DCE analysis (Tables 2, 3), suggesting that is important to use the same VIF selection method when performing perfusion analysis (see Sect. “VIF selection in DCE” paragraph).

To better clarify why these ICC values were obtained in intersoftware comparison, further analysis on the impact of different postprocessing options on data reproducibility were performed considering hypotheses and results of published studies. In particular, the impact of deconvolution algorithms on DSC and VIF selection on DCE data reproducibility were investigated.

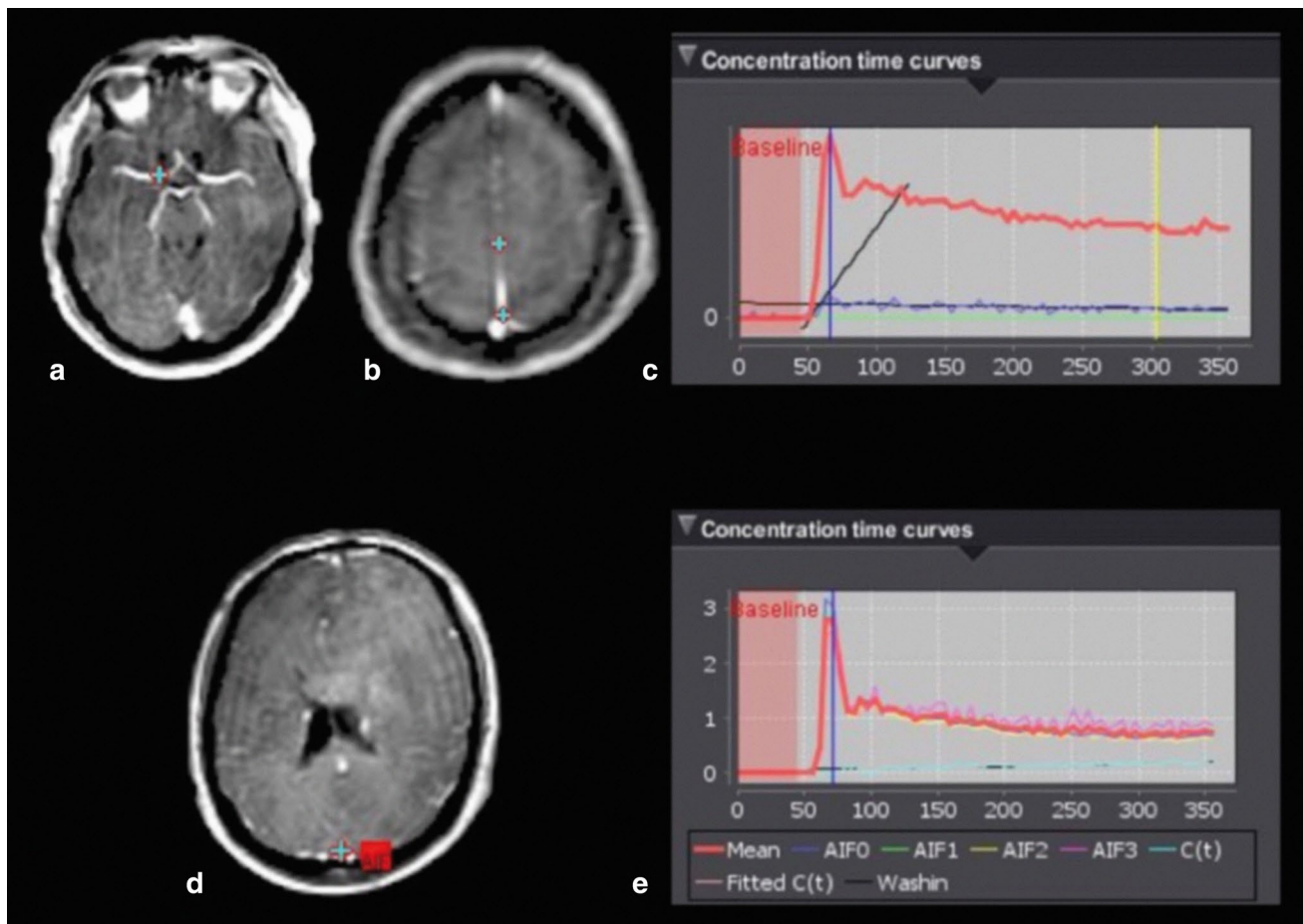


**Fig. 3** Comparison of automatic and manual VIF selection in the same patient; in this case automatic VIF selection on DCE maps shows both arterial (a) and venous (b) input; manual VIF selection on DCE maps consists in venous input only (d); c, e Concentration time

curves show different peaks, with the one derived from automatic VIF being lower. The curve derived from the manual VIF is the mean of four different input located around the pixel selected (e)

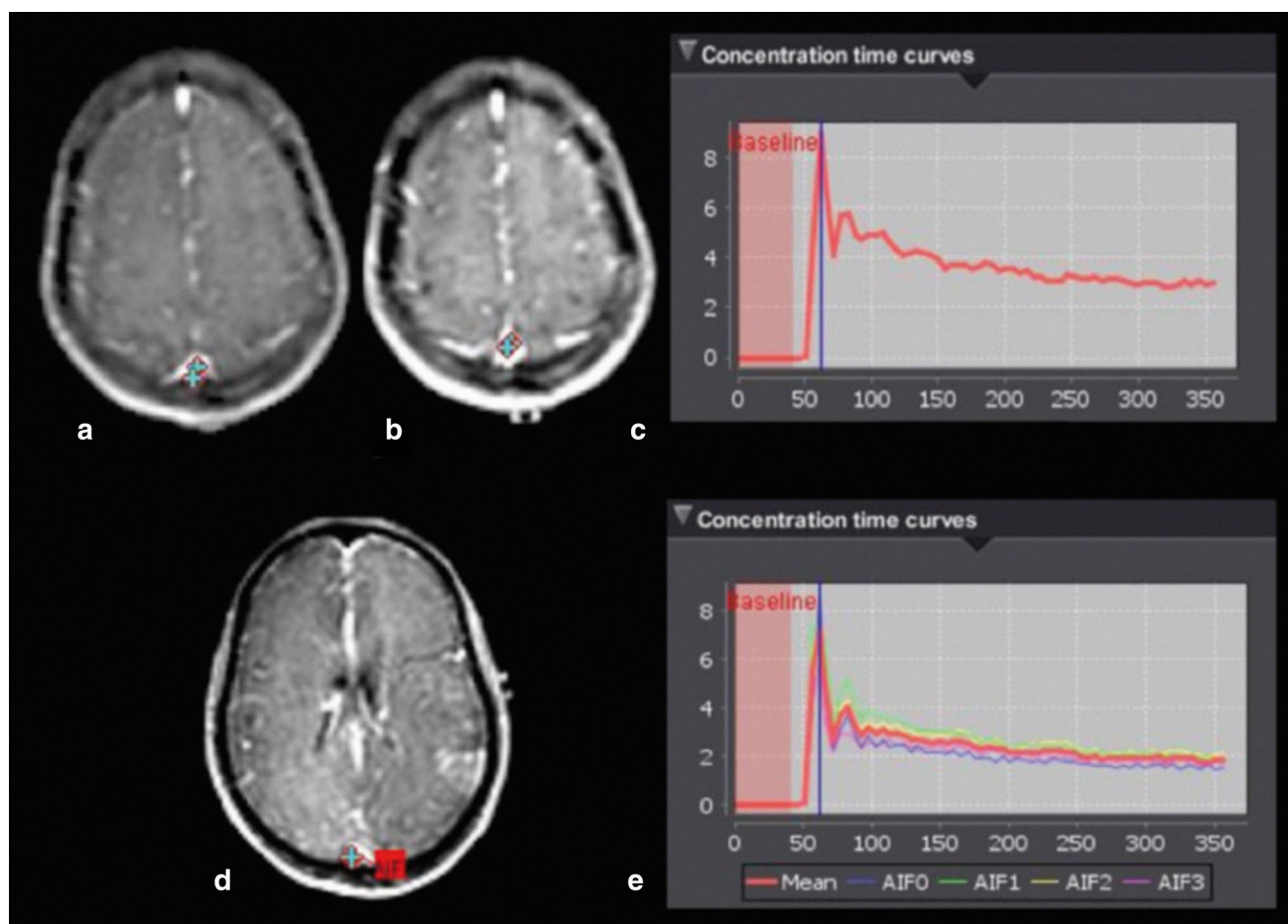


**Fig. 4** Comparison of automatic and manual VIF selection in the same patient; in this case automatic VIF selection on DCE maps shows only venous input (**a, b**); manual VIF selection on DCE maps

consists in venous input only (**d**); **c, e** Concentration time curves shows similar peaks. The curve derived from the manual VIF is the mean of four different input located around the pixel selected (**e**)

### Deconvolution algorithms in DSC

For DSC, one of the proposed factors that may affect reproducibility is the choice of the deconvolution algorithm [27, 30]. In our study DSC analyses were performed applying both different and same deconvolution algorithms in the two software, finding low intersoftware reproducibility, that only slightly increased from an ICC of 0.455–0.582 when selecting the same algorithm (sSVD) (Table 3). It is possible that the choice of a different algorithm per se does not introduce significant variability; this was proved comparing the data obtained using the two different SVD methods in the same software, resulting in an almost perfect agreement with an ICC of 0.999 (Table 4). Bland–Altman analysis confirmed this finding since the dispersion of data is very low (Fig. 1). This could mean that the two software apply the same algorithm in a different way or that the main source of variability may be due to other postprocessing options. Lastly, it must be noticed that we compared rCBV

value, while some differences are expected in CBF when comparing oSVD and sSVD [36].

### VIF selection in DCE

A possible source of variability for DCE analysis is the definition of VIF, as proposed by Heye [25] and Beuzit [28]. Our data confirms their hypothesis, since different quantitative values and thus different reproducibility of DCE data according to different VIF estimation methods were obtained. In the intersoftware comparison, a better reproducibility was obtained for both  $K^{\text{trans}}$  and  $V_p$  when the VIF was selected manually in both software (Tables 2, 3). These differences may arise due to a different vessel selection in the two methods: the automatic selection of VIF selects both arteries and veins as a source of input, and this may determine a different peak characterization of the VIF curve (Figs. 3, 4); on the other hand, when performing the manual VIF selection, only venous signal is chosen, making

the peaks of the curves probably more similar between the two software. Nevertheless, even considering this slight improvement, reproducibility still remains low. To precisely define the impact of different VIF on reproducibility, the two VIF estimation methods were compared in the same software (Figs. 3, 4). Our results show that this single change in postprocessing step has a significant impact on data as only moderate agreement was obtained, even if the ROIs were positioned in the same area and no other differences exist between the datasets compared (Table 4). Probably the VIF selection itself cannot entirely explain the poor reproducibility but it seems to play a major role in it.

Our study confirms the recent findings by Orsingher [26], Milchenko [31] and Kelm [32], who also found low intersoftware reproducibility of DSC parameter CBV. Moreover, we confirmed its good interobserver reproducibility found by Kelm [32]. Very similar findings were found for DCE parameters. This has several consequences on the application of perfusion analysis.

The excellent intrasoftware reproducibility suggests that each software can be used in a reliable way even by multiple readers. It must be said, however, that a thorough training is necessary to obtain this result and the acquisition and analysis protocol must be followed very strictly.

The poor intersoftware reproducibility and the impact of postprocessing options on data reproducibility have consequences on the design of follow-up studies, on the application of data published in literature and on the daily clinical routine use of perfusion analysis. Follow-up studies should be designed and performed using the same software and the same postprocessing options (i.e. VIF selection), otherwise it could be difficult to define if any observed variation in pharmacokinetic parameters is a true biological phenomenon or it is simply related to the chosen analysis method. Moreover, it could be risky to apply published findings to other datasets, unless the same software, analysis protocol and acquisition protocol have been used. This is particularly relevant for those studies that define cut-off values for PWI biomarkers (i.e. in tumors grading). It must be said, however, that, as shown in the work by Kelm [32], different diagnostic accuracy is unlikely to be found among different FDA-cleared software.

## Conclusions

In conclusion, we found a very good intrasoftware reproducibility and poor intersoftware reproducibility for DCE and DSC analyses, suggesting that while the use of a single software ensures reliable results, caution should be taken when comparing data obtained using different software and different postprocessing options, since the reproducibility in this case is not guaranteed anymore.

## Compliance with ethical standards

**Conflict of interest** Nicoletta Anzalone served as a consultant for Bayer HealthCare. Marcello Cadioli reports personal fees from Philips Spa and from San Raffaele Scientific Institute, outside the study. All the other authors declare that they have no potential conflict of interest.

**Ethical approval** All procedures performed in studies involving human participants were in accordance with the ethical standards of the institutional and/or national research committee and with the 1964 Helsinki declaration and its later amendments or comparable ethical standards. This article does not contain any studies with animals performed by any of the authors.

**Funding** No funding was received for this study.

**Informed consent** For this type of study formal consent is not required.

## References

1. Nguyen TB, Cron GO, Perdrizet K et al (2015) Comparison of the diagnostic accuracy of DSC- and dynamic contrast-enhanced MRI in the preoperative grading of astrocytomas. *Am J Neuroradiol* 36:2017–2022. doi:[10.3174/ajnr.a4398](https://doi.org/10.3174/ajnr.a4398)
2. Emblem K, Nedregaard B, Nome T et al (2008) Glioma grading by using histogram analysis of blood volume heterogeneity from MR-derived cerebral blood volume maps. *Radiology* 247:808–817. doi:[10.1148/radiol.2473070571](https://doi.org/10.1148/radiol.2473070571)
3. Jung SC, Yeom JA, Kim JH et al (2014) Glioma: application of histogram analysis of pharmacokinetic parameters from T1-weighted dynamic contrast-enhanced MR imaging to tumor grading. *Am J Neuroradiol* 35:1103–1110. doi:[10.3174/ajnr.A3825](https://doi.org/10.3174/ajnr.A3825)
4. Law M, Yang S, Babb J et al (2004) Comparison of cerebral blood volume and vascular permeability from dynamic susceptibility contrast-enhanced perfusion MR imaging with glioma grade. *AJNR Am J Neuroradiol* 25:746–755
5. Falk A, Fahlström M, Rostrup E et al (2014) Discrimination between glioma grades II and III in suspected low-grade gliomas using dynamic contrast-enhanced and dynamic susceptibility contrast perfusion MR imaging: a histogram analysis approach. *Neuroradiology* 56:1031–1038. doi:[10.1007/s00234-014-1426-z](https://doi.org/10.1007/s00234-014-1426-z)
6. Law M, Young R, Babb J et al (2008) Gliomas: predicting time to progression or survival with cerebral blood volume measurements at dynamic susceptibility-weighted contrast-enhanced perfusion MR imaging. *Radiology* 247:490–498. doi:[10.1148/radiol.2472070898](https://doi.org/10.1148/radiol.2472070898)
7. Schmainda KM, Prah M, Connelly J et al (2014) Dynamic-susceptibility contrast agent MRI measures of relative cerebral blood volume predict response to bevacizumab in recurrent high-grade glioma. *Neuro Oncol* 16:880–888. doi:[10.1093/neuonc/not216](https://doi.org/10.1093/neuonc/not216)
8. Piludu F, Marzi S, Pace A et al (2015) Early biomarkers from dynamic contrast-enhanced magnetic resonance imaging to predict the response to antiangiogenic therapy in high-grade gliomas. *Neuroradiology* 57:1269–1280. doi:[10.1007/s00234-015-1582-9](https://doi.org/10.1007/s00234-015-1582-9)
9. Kim R, Choi S, Yun T et al (2016) Prognosis prediction of non-enhancing T2 high signal intensity lesions in glioblastoma patients after standard treatment: application of dynamic



- contrast-enhanced MR imaging. *Eur Radiol*. doi:10.1007/s00330-016-4464-6
10. Khalifa J, Tensaouti F, Chaltiel L et al (2016) Identification of a candidate biomarker from perfusion MRI to anticipate glioblastoma progression after chemoradiation. *Eur Radiol*. doi:10.1007/s00330-016-4234-5
  11. Sanz-Requena R, Revert-Ventura A, Martí-Bonmati L et al (2013) Quantitative MR perfusion parameters related to survival time in high-grade gliomas. *Eur Radiol* 23:3456–3465. doi:10.1007/s00330-013-2967-y
  12. Yoon R, Kim H, Paik W et al (2016) Different diagnostic values of imaging parameters to predict pseudoprogression in glioblastoma subgroups stratified by MGMT promoter methylation. *Eur Radiol*. doi:10.1007/s00330-016-4346-y
  13. Larsen V, Simonsen H, Law I et al (2012) Evaluation of dynamic contrast-enhanced T1-weighted perfusion MRI in the differentiation of tumor recurrence from radiation necrosis. *Neuroradiology* 55:361–369. doi:10.1007/s00234-012-1127-4
  14. Wang S, Martinez-Lage M, Sakai Y et al (2015) Differentiating tumor progression from pseudoprogression in patients with glioblastomas using diffusion tensor imaging and dynamic susceptibility contrast MRI. *Am J Neuroradiol* 37:28–36. doi:10.3174/ajnr.A4474
  15. Thomas AA, Arevalo-Perez J, Kaley T et al (2015) Dynamic contrast enhanced T1 MRI perfusion differentiates pseudoprogression from recurrent glioblastoma. *J Neurooncol* 125:183–190. doi:10.1007/s11060-015-1893-z
  16. Prager AJ, Martinez N, Beal K et al (2015) Diffusion and perfusion MRI to differentiate treatment-related changes including pseudoprogression from recurrent tumors in high-grade gliomas with histopathologic evidence. *Am J Neuroradiol* 36:877–885. doi:10.3174/ajnr.A4218
  17. Heye AK, Culling RD, Hernández MDCV et al (2014) Assessment of blood-brain barrier disruption using dynamic contrast-enhanced MRI. a systematic review. *Neuroimage Clin* 6:262–274. doi:10.1016/j.nicl.2014.09.002
  18. Ellingson B, Bendszus M, Sorensen G, Pope W (2014) Emerging techniques and technologies in brain tumor imaging. *Neuro Oncol* 16:vii12–vii23. doi:10.1093/neuonc/nou221
  19. Shiroishi M, Boxerman J, Pope W (2015) Physiologic MRI for assessment of response to therapy and prognosis in glioblastoma. *Neuro Oncol*. doi:10.1093/neuonc/nov179
  20. Usinskiene J, Ulyte A, Bjørnerud A et al (2016) Optimal differentiation of high- and low-grade glioma and metastasis: a meta-analysis of perfusion, diffusion, and spectroscopy metrics. *Neuroradiology*. doi:10.1007/s00234-016-1642-9
  21. Goh V, Schaeffter T, Leach M (2013) Reproducibility of dynamic contrast-enhanced MR imaging: why we should care. *Radiology*. doi:10.1148/radiol.12122447
  22. Viallon M, Cuvinciu V, Delattre B et al (2015) State-of-the-art MRI techniques in neuroradiology: principles, pitfalls, and clinical applications. *Neuroradiology* 57:441–467. doi:10.1007/s00234-015-1500-1
  23. DCE-MRI Technical Committee (2012) DCE-MRI quantification profile, quantitative imaging biomarkers alliance. Version 1.0. Publicly Reviewed Version. QIBA. <http://RSNA.org/QIBA>
  24. Welker K, Boxerman J, Kalnin A et al (2015) ASFN recommendations for clinical performance of MR dynamic susceptibility contrast perfusion imaging of the brain. *AJNR Am J Neuroradiol* 36:E41–E51. doi:10.3174/ajnr.A4341
  25. Heye T, Davenport M, Horvath J et al (2013) Reproducibility of dynamic contrast-enhanced MR imaging. Part I. Perfusion characteristics in the female pelvis by using multiple computer-aided diagnosis perfusion analysis solutions. *Radiology* 266:801–811. doi:10.1148/radiol.12120278
  26. Orsingher L, Piccinini S, Crisi G (2014) Differences in dynamic susceptibility contrast MR perfusion maps generated by different methods implemented in commercial software. *J Comput Assist Tomogr* 38:647–654. doi:10.1097/RCT.0000000000000115
  27. Kudo K, Sasaki M, Yamada K et al (2010) Differences in CT perfusion maps generated by different commercial software: quantitative analysis by using identical source data of acute stroke patients I. *Radiology*. doi:10.1148/radiol.254082000
  28. Beuzit L, Eliat P-AA, Brun V et al (2015) Dynamic contrast-enhanced MRI: study of inter-software accuracy and reproducibility using simulated and clinical data. *J Magn Reson Imaging*. doi:10.1002/jmri.25101
  29. Goh V, Shastry M, Engledow A et al (2010) Commercial software upgrades may significantly alter perfusion CT parameter values in colorectal cancer. *Eur Radiol* 21:744–749. doi:10.1007/s00330-010-1967-4
  30. Kudo K, Christensen S, Sasaki M et al (2013) Accuracy and reliability assessment of CT and MR perfusion analysis software using a digital phantom. *Radiology* 267:201–211. doi:10.1148/radiol.12112618
  31. Milchenko M, Rajderkar D, LaMontagne P et al (2014) Comparison of perfusion- and diffusion-weighted imaging parameters in brain tumor studies processed using different software platforms. *Acad Radiol* 21:1294–1303. doi:10.1016/j.acra.2014.05.016
  32. Kelm ZS, Korfiatis PD, Lingineni RK, Daniels JR, Buckner JC, Lachance DH, Parney IF, Carter RE, Erickson BJ (2015) Variability and accuracy of different software packages for dynamic susceptibility contrast magnetic resonance imaging for distinguishing glioblastoma progression from pseudoprogression. *J Med Imaging (Bellingham)* 2(2):026001
  33. Tofts PS, Brix G, Buckley DL et al (1999) Estimating kinetic parameters from dynamic contrast-enhanced T(1)-weighted MRI of a diffusible tracer: standardized quantities and symbols. *J Magn Reson Imaging* 10:223–232
  34. Mouridsen K, Christensen S, Gyldensted L, Østergaard L (2006) Automatic selection of arterial input function using cluster analysis. *Magn Reson Med* 55:524–531. doi:10.1002/mrm.20759
  35. Østergaard L, Sorensen A, Kwong K et al (1996) High resolution measurement of cerebral blood flow using intravascular tracer bolus passages. Part II: experimental comparison and preliminary results. *Magnet Reson Med* 36:726–736. doi:10.1002/mrm.1910360511
  36. Wu O, Østergaard L, Weisskoff RM et al (2003) Tracer arrival timing-insensitive technique for estimating flow in MR perfusion-weighted imaging using singular value decomposition with a block-circulant deconvolution matrix. *Magn Reson Med* 50:164–174. doi:10.1002/mrm.10522